Macquarie Island Cloud and Radiation Experiment (MICRE)
Final Report

February 28, 2020
Principal Investigator: Roger Marchand, University of Washington

Overview -

The U.S. Department of Energy Atmospheric Radiation Measurement (ARM) program, the Australian Antarctic Division (AAD) and the Australian Bureau of Meteorology (BoM) collaborated in deploying a variety of ground-instrumentation to Macquarie Island between March 2016 and March 2018. Macquarie Island is located at 54.5° S, 158.9° E and is well situated for studying clouds over the Southern Ocean. The primary objective of the March 2016 to March 2018 deployment, hereafter the Macquarie Island Cloud and Radiation Experiment (MICRE), was to collect observations of surface radiation, cloud, precipitation, and aerosol properties.

This report provides a description of the instruments deployed and datasets collected, along with a summary of key data quality issues and information on some value-added-products that are being constructed to assist scientist in making use of the data.

Table of Contents

1.0 Introduction:

Clouds over the Southern Ocean (SO) differ from those over the Northern Hemisphere oceans, with low altitude supercool clouds being more ubiquitous over the Southern Ocean (SO) [Mace et al. 2009, 2010, Huang et al. 2016]. Global climate model (GCM) simulations [Trenberth and Fasullo 2010] and reanalysis products [Naud et al. 2014] struggle to represent these clouds, and in recent years, a lack of low cloud over the Southern Ocean, primarily in the cold sector of cyclonic systems, has been found to result in large radiative errors in both climate models and reanalysis [Williams et al. 2013; Naud et al. 2014, Bodas-Salcedo et al. 2014, 2016, Kay et al 2016]. These cloud radiative errors result in significant errors in the surface energy budget and excess heat uptake by the ocean surface [Sallée et al. 2013, Schneider and Reusch 2016], and are of profound importance to global climate, including influencing the position of the Southern Hemisphere midlatitude jet, the Inter-Tropical Convergence Zone (ITCZ) position, cross-hemispheric energy transports [Ceppi et al. 2012, 2013, Hwang and Frierson 2013, Kay et al 2016], and even SO cloud feedbacks and global climate sensitivity [Gettelman et al 2019b, Bodas-Salcedo et al 2019]. In addition, the remoteness of the SO from anthropogenic and natural continental aerosol sources makes the SO a unique venue to improve our understanding of cloud aerosol interactions, and the role of marine biogenic aerosols and their precursors. Despite the importance and the challenge of simulating cloud and aerosol effects over the SO, there have been only sparse and infrequent observations in this region. Observations are sorely needed to improve process level understanding of atmospheric processes, and their representations in models.

In response to the need for additional measurements of surface radiative fluxes, as well as cloud, precipitation, and aerosol properties over the Southern Ocean, the U.S. Department of Energy Atmospheric Radiation Measurement (ARM) program, the Australian Antarctic Division (AAD) and the Australian Bureau of Meterology (BoM) collaborated in deploying a variety of ground-instrumentation to Macquarie Island between March 2016 and March 2018. Macquarie Island is located at 54.5° S, 158.9° E and has a small research station operated by the Australian Antarctic Division (AAD) that is staffed year-round, in part by the Australian Bureau of Meteorology (BoM). The station supports a variety of research activities and includes a long history of surface weather and radiosonde observations [Hande et al. 2012, Wang et al. 2015].

The primary objective of the March 2016 to March 2018 deployment, hereafter the Macquare Island Cloud and Radiation Experiment (MICRE) was to collect observations of surface radiation, cloud, precipitation, and aerosol properties. These could then be used evaluate satellite datasets, improve knowledge of diurnal and seasonal variations in cloud and aerosol properties (especially as pertains to the vertical structure of boundary layer clouds, precipitation, and the pervasive supercool liquid clouds which occupy this region), and eventually enable more detailed modeling studies that will improve model representations key aerosol, cloud and precipitation processes.

MICRE is part of a set of coordinated Southern Ocean experiments. Specifically the aircraft-based Southern Ocean Clouds, Radiation, Aerosol Transport Experimental Study

(SOCRATES) and ship-based Measurements of Aerosols Radiation and CloUds over the Southern Oceans (MARCUS) and Australian funded Clouds, Aerosols, Precipitation, Radiation, and atmospherIc Composition Over the southeRn oceaN (CAPRICORN) II projects. The key contribution that MICRE makes to this collection of experiments derives from its longer duration, which provides a longer sampling interval for the evaluation of satellite data and a seasonal and diurnal context from which to understand the aircraft and ship-based observations.

2.0 Instrumentation

Instruments deployed during MICRE (by BoM, AAD, ARM and some additional individual investigators) are listed in Table 1. In short, the observational data includes (i) observations of passive surface radiation (solar, longwave, microwave), (ii) precipitation rain rates, types and particle size from a precipitation disdrometer (iii) cloud radar reflectivity and Dopper velocity, along with ceilometer and lidar backscatter (including depolarization) which provide information on cloud occurrence, cloud-base height, cloud & precipitation particle size and phase, and (iv) surface measurements of total aerosol number concentration, cloud condensation number concentration, and ice nucleating particle (INP) number concentration from contributors Ruhi Humphries and Paul DeMott.

Data from all ARM instruments is available through the ARM data archive. Data from non-ARM instruments, as well as many derived fields from the PI (Dr. Marchand) and contributing investigators at BoM and AAD, will eventually be available through the ARM archives as PI Value-Added-Products (VAPs). However, as of the time this report is being written, these VAP data are still being developed. Developmental versions of these data are publicly available to interested users on Dr. Marchand's web site. Details on the VAP contents are given in Section 4.

Table 1 – MICRE Instruments. Dates listed for each instrument denote periods for which high quality data is generally available, though all instruments have occasional "drop outs" where data is missing or of poor quality for a few hours or days. "PC:" denotes the primary contact for non-ARM instruments "ARM:" denotes the name of the ARM datastream (which can be used to quickly find these data in the ARM archive).

MICRE Instrumentation	Data Availability	References/Notes
94 GHz Cloud Radar (BASTA)	20160402 - 20170317 (First year only)	Delanoë et al. [2016] Mace and Protat [2018] PC: Alain Protat (BOM)
AAD **Polarization Lidar**	20160407 - 20161127 20170401 - 20180313	See note 1 PC: Simon Alexander (AAD)
Vaisala **Ceilometer** ARM U. Canterbury	 20160402 - 20161214 20170222 - 20180313 20160402 - 20180313	Vaisala Model CT25K Münkel et al. 2007 ARM: mcqceilS1.b1 PC: Adrian McDonald (UC)

Microwave Radiometers: ARM **3 channel** ARM **2 channel**	 20160402 - 20160613 20161228 - 20180313	Cadeddu et al. 2013 See note 2
ARM **Disdrometer** (OTT PARSIVEL2)	20160402 - 20180313 (see note 3)	Angulo-Martínez et al. 2018 ARM: mcqpars2S1.b1
Broadband **SW & LW fluxes** (SKYRAD, GRDRAD) **CIMEL sun photometer** **Multi-Filter Rotating Shadowband Radiometer (MFRSR)**	20160403 - 20180313 (LW see notes 4, 5) 20160403 - 20180311 Failed (see note 6) 20160321 - 20160810 20160915 - 20180313	Andreas et al. 2018 ARM: mcqskyrad60sS1.b1, mcqgndrad60sS1.b1 Holben et al. 1998 ARM: mcqcsphot ARM: mcqmfrsrS1
Other Data **Surface INP Filter Samples** **Surface CPC & CCN** **BOM Radiosondes** **AAD Surface Met**	 2nd Year only Both years Both years Both years	 Two week samples DeMott et al. 2018 PC: Ruhi Humphries Twice per day, 0 and 12 UTC PC: Simon Alexander (AAD)

Table Notes:

1: The AAD-Lidar failed in Fall of 2016. The instrument was fixed and redeployed in Spring 2017. Calibration issues (primarily with depolarization) remain and are under study.

2: LWP and PWV retrieved via physical-iterative technique [Marchand et al. 2003] is included in the CPP-VAP product (Section 4). Raw brightness temperatures are in ARM archive but be aware that there is some unusual interference noise with these data (Section 3). For 3-channel MWR this raw data are only instrument-level files (not NetCDF). Current plans are for the ARM standard MWRRET retrieval to be run on the 2-channel data.

3: For unknown reasons the PARSIVEL reset to a previous output mode starting on 20161031 that was incompatible with the ARM ingest. This resulted in bad/corrupt data in several fields. Most notably this included the precipitation rate, liquid water content, total number of particles, and weather codes (DQR D170524.7 / DPQR 6227). In general the PARSIVEL vendor's algorithm did not work well during MICRE and additional processing was undertaken by Marchand and Tansey (see section 4).

4: Upwelling and downwelling LW fluxes are biased or bad from start of experiment until 20060815. Upwelling LW is suspect for several more weeks until 20160908, but downwelling is fine after 20060815.

5: Two radiometers for broadband LW were deployed. The measurements by the two radiometers agree well except in two time windows, where radiometer 2 has a value that is 2% lower than radiometer 1 and appears to be incorrect.

6: MFRSR collected data for much of the experiment, but the rotating shadow band was not initially aligned well and the rotating band eventually failed completely. Narrowband radiances during cloudy period might be used but the data are uncalibrated because of the inability to carry out a Langley analysis. Use with great caution.

3.0 Overview of ARM Instrument Data Quality

Much of the ARM instrumentation was operational by April 4, 2016. But all of the instruments suffered some difficulties or down time during the experiment, and in several cases instruments had to be replaced during the Fall or Spring resupply voyages. Users of the instrument-level data are advised to read associated ARM instrument data quality reports. A variety of key issues are noted at the bottom of table #1. In this section, we discuss further some additional issues related to the MWR and PARSIVEL disdrometer.

<u>*Passive Microwave Radiometer (MWR)*</u>
The MWR data record is perhaps the most problematic of the ARM datasets. Both a 2-channel and a 3-channel radiometer were deployed to Macquarie. The 2-channel failed on arrival. The 3-channel worked initially, but it also failed on June 13 2016. A second 2-channel instrument was deployed as part of the November of 2106 resupply (the island is resupplied only twice a year). Problems with the power supply stability (ground faults) resulted in limited data collection by the replacement until near the end of December (12/28/2016). But once these problems were solved the instrument worked admirably until the end of the deployment in March 2018.

However, all MWR measurements suffered from *Interference from an unknown source that caused periodic spikes in the measurements.* The spikes occurred in measurements at all frequencies (23, 30 & 89 GHz). An example is shown below in Figure #1. While the spikes are obvious during periods with little cloud water (e.g. on the right half of the figure in the top panel) they are difficult to see during periods with significant variation in cloud water (i.e. on the right half). However the spikes are regularly spaced, and PI Marchand developed a filter to remove the spikes from retrievals for cloud liquid water path and precipitable water vapor.

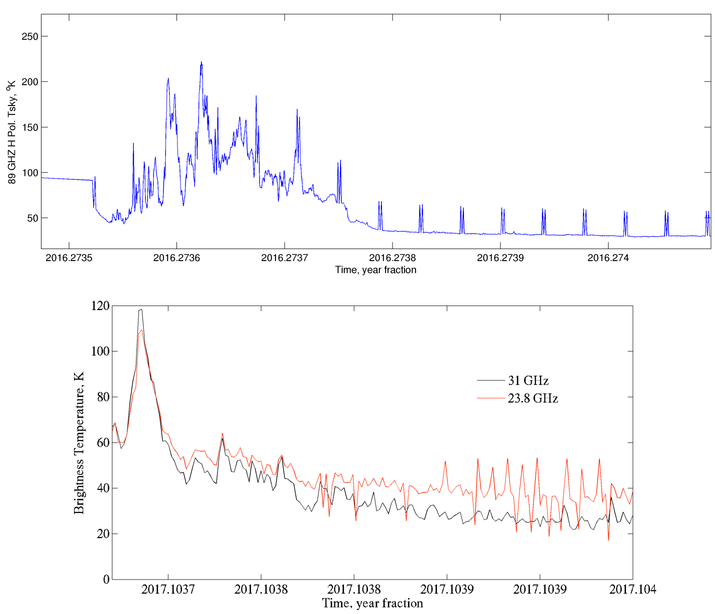

Figure #1 – Example of noise spikes in 3-channel 89 GHz (top) and 2–channel data (bottom)

PARSIVEL Laser Disdrometer

The PARSIVEL disdrometer did not function particularly well during MICRE. The data were found to have considerable wind-driven artifacts and did not preform well during periods with solid (ice) or mixed-phase precipitation. It appears that the manufacture's algorithms treat all precipitation as liquid phase. In addition, for unknown reasons the PARSIVEL reset to an unexpected output mode on 20161031 that was incompatible with the ARM data logger configuration. This resulted in bad/corrupt data in several fields, which was not noticed at the time. Most notably this included the precipitation rate, liquid water content, total number of particles, and weather codes (which contain information on the precipitation type).

Consequently, considerable effort has been devoted by University of Washington Graduate Student Emily Tansey in developing an improved algorithm called "Parsivel Improved Rate and Type" or PIRAT. The algorithm is undergoing final development work now and publication of results is expected in the next few months. The PIRAT data are included in the Value Added Products described below.

4.0 Value Added Products

Under support from the ASR program and as part of the MARCUS and MICRE campaigns, an *Environmental Parameters Value-Added-Product (EP-VAP)* as well as a *Cloud and Precipitation Parameters Value-Added-Product (CPP-VAP)* is being generated. The purpose of this value added dataset is to advance scientific studies associated with the MARCUS and MICRE campaigns, as well as providing a vehicle to ensure that NON-ARM datasets are data quality controlled and archived by ARM.

Work on these VAPS is not complete. In particular, for the CPP-VAP the plan is to include cloud-base and sub-cloud precipitation phase (liquid vs. ice) based on lidar-depolarization measurements, and potentially day-time cloud microphysics based on microwave radiometer and broadband SW fluxes. We hope to have the depolarization-based phase, soon. And for EP-VAP the plan is to include some aerosol fields, which are not yet in place. For MICRE this will include only surface CCN and CN counts. These data were received by the PI only in the past month and have not yet been quality controlled.

The next two subsections list the contents of each VAP (as it stands presently). When completed these VAP products will be placed in the ARM archive, but for now developmental versions are available via PI Marchand's web site at the link below. This site also contains documentation describing the contents (and retrieval techniques) in greater detail.

https://atmos.uw.edu/~roj/nobackup/MARCUS_and_MICRE/

4.1 CPP-VAP

The contents of the VAP are listed in Table #2. The data is organized by **DATA_SOURCE** (defined as an instrument or retrieval) where the data source is in capital letters and the associated variables are in small letters. So for example the data file contains the variable "RADAR_time_gmt" which is the time of day (in gmt hours) associated with all the RADAR variables. Many but not all of the variables are tied to the radar time-grid.

Please note that **most of the DATA_SOURCE categories have a data_quality field**. This is a bit-packed variable, where a value of 0 means "no known problems or concerns" and all other values mean there is a potential problem or concern. The file metadata explains what each bit in the data_quality field. Additional details on the retrievals are given in the online documentation.

Table #2 – Contents of CP-VAP file. Units and other metadata are included in the NetCDF file.

DATA SOURCE	Variables	Notes:
RADAR Radar Measurements	time_gmt data_quality_flag height reflectivity_masked mean_Doppler_velocity	Radar data has been processed to remove coupling artifacts and clutter.
RADAR_LIDAR_BOUNDARIES Boundaries from combination of radar, ARM ceilometer and UC ceilometer	time_gmt data_qualtity_flag n_layers (number of layers) layer_type (radar only, lidar only, both) layer_radar_base layer_radar_top layer_median_lidar_base n_ceilometer_columns n_ceilometer_columns_obsercured	Time sampling matches radar (~12s) when radar was running, otherwise 60s. Lidar boundaries are smoothed to 1 minute scale.
ZV_PRECIP_RETRIEVAL Near surface precipitation based on radar reflectivity (Z) and mean Doppler velocity (V)	time_gmt near_surface_data_quality_flag near_surface_max_reflecitity near_surface_max_precip_rate near_surface_max_precip_effective_radius	Near surface mean 250 to 500 m above the surface but also below cloud base. Retrieval is not undertaken when cloud-base is below 350m (see quality flag)
MWR_RETRIEVAL Retrieval uses radiosondes profiles and radar-lidar-boundaries, in addition to MWR brightness temperatures.	time_gmt data_quality_flag liquid_water_path (LWP) precipitable_water_vapor (PWV) hours_to_sonde n_layers tb23 (measured value) tb31 (measured value)	Based on an iterative technique that tries to adjust LWP and PWV so forward calculated value of brightness temperatures (tb) matches observed

	calculated_tb23 (retrieved value) calculated_tb31 (retrieved value)	values.
Z_LWP_CLOUD_RETRIEVAL Retrieved cloud microphysics for ***non-precipitation*** liquid clouds ONLY.	time_gmt data_quality_flag droplet_number_concentration column_effective_radius (LWC-weighted)	
SURFACE_MET Automated surface meteorological station data	time_gmt temperature pressure relative_humidity wind_speed wind_direction accumulated_rainfall	accumulated_rainfall is based on tipping bucket, since the start of the UTC day.
PARSIVEL Parsivel surface disdrometer VENDOR retrievals (not recommended)	time_gmt vendor_precip_rate vendor_precip_effective_radius	Neither the Parsivel's measurements nor vendor's retrievals are optimal for Macquarie. We will likely remove these data in future versions.
PARSIVEL_PIRAT Parsivel Improved Rate and Type (PIRAT) retrieval	time_gmt (fixed five minute grid) precip_type_best precip_type_metrics precip_rate_best precip_rate_by_type precip_effective_radius bin_particle_size bin_velocity spectrum_raw spectrum_corrected	Temporal sampling rate is reduce to 5 minutes to improve S/N, and includes various corrections (see section 2). Data includes raw and corrected Drop Size-Velocity Spectra.
SURF_RAD Surface broadband shortwave and longwave fluxes	time_gmt shortwave_down_total shortwave_down_direct shortwave_down_diffuse shortwave_up_total longwave_down longwave_up	

4.2 EP-VAP

This products merges measurements and derived products obtained from both ARM and other sources. The files contain the quantities listed below, at the location of the AA or at Macquaire Island at 10-min resolution. A more detailed description of the file contents is provided in the online documentation.

EP-VAP parameters:

(i) Basic time and location information

(ii) Local meteorological conditions including:
sea surface temperature (SST), lower tropospheric stability (LTS), marine cold air outbreak (MCAO) index, inversion height, and lifting condensation level (LCL).

(iii) Location relative to the oceanic polar front (PF), center of the closest cyclone, and nearest warm fronts and cold fronts

(iv) Location of air parcels 72 hours prior to its arrival at/above the ship computed using the HYSPLIT back trajectory model

(v) Aerosol Properties (*TBD, still under construction but will include CN and CCN*).

(vi) Cloud & Precipitation Properties, including:
Cloud base/top height, and cloud base/top temperature (precip. fields are not included yet).

(vii) Coincident cloud properties retrieved from the Himawari-8 satellite including:
cloud fraction, cloud base/top height, cloud top temperature, cloud top pressure, liquid water path, optical depth, cloud effective radius, cloud droplet number concentration.

References

Andreas, Afshin, Dooraghi, Mike, Habte, Aron, Kutchenreiter, Mark, Reda, Ibrahim, and Sengupta, Manajit, 2018: Solar Infrared Radiation Station (SIRS), Sky Radiation (SKYRAD), Ground Radiation (GNDRAD), and Broadband Radiometer Station (BRS) Instrument Handbook, doi:10.2172/1432706.

Angulo-Martínez, M., Beguería, S., Latorre, B., and Fernández-Raga, M.: Comparison of precipitation measurements by OTT Parsivel2 and Thies LPM optical disdrometers, 2018: *Hydrol. Earth Syst. Sci*., 22, 2811–2837, doi: 10.5194/hess-22-2811-2018.

Bodas-Salcedo, A., K. Williams, M. Ringer, I. Beau, J. Cole, J. Dufresne, T. Koshiro, B. Stevens, Z. Wang, and T. Yokohata, 2014: Origins of the solar radiation biases over the Southern Ocean in CFMIP2 models. J. Climate, doi:10.1175/JCLI-D-13-00169.1.

Bodas-Salcedo, A., T. Andrews, A.V. Karmalkar, and M.A. Ringer, 2016: Cloud liquid water path and radiative feedbacks over the Southern Ocean. Geophys. Res. Lett., 43, 10938-10946, doi:10.1002/2016GL070770.

Bodas-Salcedo, A., J. P. Mulcahy, T. Andrews, K. D. Williams, M. A. Ringer, P. R. Field, and G. S. Elsaesser. 2019. "Strong Dependence of Atmospheric Feedbacks on Mixed-Phase Microphysics and Aerosol-Cloud Interactions in HadGEM3." Journal of Advances in Modeling Earth Systems 11 (6): 1735–58, doi:10.1029/2019MS001688.

Cadeddu, M. P., Liljegren, J. C., and Turner, D. D., 2013: The Atmospheric radiation measurement (ARM) program network of microwave radiometers: instrumentation, data, and retrievals, Atmos. Meas. Tech., 6, 2359–2372, doi: 10.5194/amt-6-2359-2013.

Ceppi, P., Y.-T. Hwang, D. M. W. Frierson and D.L. Hartmann, 2012: Southern Hemisphere jet latitude biases in CMIP5 models linked to shortwave cloud forcing. Geophys. Res. Lett., doi:10.1029/2012GL053115.

Ceppi, P., M. D. Zelinka, and D. L. Hartmann, 2014: The response of the Southern Hemispheric eddy-driven jet to future changes in shortwave radiation in CMIP5, Geophys. Res. Lett., 41, 3244–3250, doi:10.1002/2014GL060043.

Delanoë, J., A. Protat, J. Vinson, W. Brett, C. Caudoux, F. Bertrand, J. Parent du Chatelet, R. Hallali, L. Barthes, M. Haeffelin, and J. Dupont, 2016: BASTA: A 95-GHz FMCW Doppler Radar for Cloud and Fog Studies. J. Atmos. Oceanic Technol., 33, 1023–1038, doi: 10.1175/JTECH-D-15-0104.1.

DeMott, PJ, T Hill, R Marchand,and S Alexander, 2018: "Macquarie Island Cloud and Radiation Experiment (MICRE) Ice Nucleating Particle Measurements Field Campaign Report". United States. https://www.osti.gov/servlets/purl/1489359.

Frisch, A.S., C.W. Fairall, and J.B. Snider, 1995: Measurement of Stratus Cloud and Drizzle Parameters in ASTEX with a Kα-Band Doppler Radar and a Microwave Radiometer. J. Atmos. Sci., 52, 2788–2799, doi:10.1175/1520-0469(1995)052<2788:MOSCAD>2.0.CO;2.

Hande, L. B., S. T. Siems, M. J. Manton, and D. Belusic (2012), Observations of wind shear over the Southern Ocean, J. Geophys. Res., 117, D12206, doi:10.1029/2012JD017488.

Holben, B. N., Eck, T. F., Slutsker, I., Tanré, D., Buis, J. P., Setzer, A., Vermote, E., Reagan, J. A., Kaufman, Y. J., Nakajima, T., Lavenu, F., Jankowiak, I., & Smirnov, A. (1998). AERONET—A federated instrument network and data archive for aerosol characterization. Remote Sensing of Environment, 66(1), 1‑16. doi: 10.1016/S0034‑4257(98)00031‑5.

Hu, Y., S. Rodier, K. Xu, W. Sun, J. Huang, B. Lin, P. Zhai, and D. Josset, 2010: Occurrence, liquid water content, and fraction of supercooled water clouds from combined CALIOP / IIR / MODIS measurements. J. Geophys. Res., 115, D00H34, doi: 10.1029/2009JD012384.

Huang, Y., S.T. Siems, M.J. Manton, D. Rosenfeld, R. Marchand, G.M. McFarquhar, and A. Protat, 2016: What is the role of sea surface temperature in modulating cloud and precipitation properties over the Southern Ocean? J. Climate, 29, 7453-7476. doi: 10.1175/JCLI-D-15-0768.1.

Hwang, Y.-T., and D.M.M. Frierson, 2013: Link between the double-Intertropical Convergence Zone problem and cloud biases over the Southern Ocean. Proc. Natl. Acad. Sci., 110, 4935-4940. doi: 10.1073/pnas.1213302110

Gettelman, A., Truesdale, J. E., Bacmeister, J. T., Caldwell, P. M., Neale, R. B., Bogenschutz, P. A., & Simpson, I. R. (2019a). The Single Column Atmosphere Model version 6 (SCAM6): Not a scam but a tool for model evaluation and development. Journal of Advances in Modeling Earth
Systems, 11, 1381–1401, doi: 10.1029/2018MS001578.

Gettelman, A., Hannay, C., Bacmeister, J. T., Neale, R. B., Pendergrass, A. G., Danabasoglu, G., et al. (2019b). High climate sensitivity in the Community Earth System Model Version 2 (CESM2). Geophysical Research Letters, 46, 8329– 8337, doi: 10.1029/2019GL083978.

Kay, J.E., C. Wall, V. Yettella, B. Medeiros, C. Hannay, P. Caldwell, and C. Bitz, 2016: Global climate impacts of fixing the Southern Ocean shortwave radiation bias in the Community Earth System Model (CESM). J. Climate, 29, 4617-4636, doi: 10.1175/JCLI-D-15-0358.1.

Mace, G. G., Q. Zhang, M. Vaughan, R. Marchand, G. Stephens, C. Trepte, and D. Winker (2009), A description of hydrometeor layer occurrence statistics derived from the first year of merged Cloudsat and CALIPSO data, J. Geophys. Res., 114, D00A26, doi:
10.1029/2007JD009755.

Mace, G.G., 2010: Cloud properties and radiative forcing over the maritime storm tracks of the Southern Ocean and North Atlantic derived from A-Train, J. Geophys. Res., 115, D10201, doi:10.1029/2009JD012517.

Mace, G.G., and A. Protat, 2018: Clouds over the Southern Ocean as observed from the R/V Investigator during CAPRICORN: Part I: Cloud occurrence and phase partitioning, J. Appl. Meteor. Clim., 57, 1783-1804, doi:10.1175/JAMC-D-17-0194.1.

Münkel, C., Eresmaa, N., Räsänen, J. et al. Boundary-Layer Meteorol (2007) 124: 117, doi: 10.1007/s10546-006-9103-3.

Naud, C., J. F. Booth, and A. D. Del Genio, 2014: Evaluation of ERA-Interim and MERRA cloudiness in the Southern Oceans. J. Climate, 27, 2109-2124.

Orr, B.W. and R.A. Kropfli, 1999: A Method for Estimating Particle Fall Velocities from Vertically Pointing Doppler Radar. J. Atmos. Oceanic Technol., 16, 29–37, 10.1175/1520-0426(1999)016<0029:AMFEPF>2.0.CO;2

Sallée, J.-B., E. Shuckburgh, N. Bruneau, A. J. S. Meijers, T. J. Bracegirdle, Z. Wang, and T. Roy (2013), Assessment of Southern Ocean water mass circulation and characteristics in CMIP5 models: Historical bias and forcing response, J. Geophys. Res. Oceans, 118, 1830–1844, doi:10.1002/jgrc.20135.

Schneider, D.P. and D.B. Reusch, 2016: Antarctic and Southern Ocean Surface Temperatures in CMIP5 Models in the Context of the Surface Energy Budget. J. Climate, 29, 1689–1716, doi: 10.1175/JCLI-D-15-0429.1

Wang, Z., S.T. Siems, D. Belusic, M.J. Manton, and Y. Huang, 2015: A Climatology of the Precipitation over the Southern Ocean as Observed at Macquarie Island. J. Appl. Meteor. Climatol., 54, 2321–2337, doi: 10.1175/JAMC-D-14-0211.1.

Williams, K.D., A. Bodas-Salcedo, M. Deque, S. Fermepin, B. Medeiros, M. Watanabe, C. Jakob, S.A. Klein, C.A. Senior, and D.L. Williamson, 2013: The Transpose-AMIP II experiment and its application to the understanding of Southern Ocean cloud biases in climate models. J. Climate, 26, 3258-3274.